CRISPRa-mediated *Kcna1* upregulation decreases neuronal excitability and suppresses seizures in a rodent model of temporal lobe epilepsy

Gaia Colasante[2#], Yichen Qiu[1#], Claudia Di Berardino[2], Luca Massimino[2], Jonathan Cornford[1], Albert Snowball[1], Steffan P. Jones[1], Serena Giannelli[2], Andreas Lieb[1], Stephanie Schorge[1,4*], Dimitri M. Kullmann[1], Vania Broccoli[2,3*], Gabriele Lignani[1*]

[1] Department of Clinical and Experimental Epilepsy, UCL Institute of Neurology, University College London, London, UK

[2] San Raffaele Scientific Institute, Via Olgettina 58, 20132, Milan, Italy

[3] CNR Institute of Neuroscience, Via Vanvitelli 32, 20129, Milan, Italy

[4] Department of Pharmacology, UCL School of Pharmacy, University College London, London, UK

[#] same contribution

* To whom correspondence should be addressed:

Gabriele Lignani g.lignani@ucl.ac.uk

Vania Broccoli v.broccoli@hsr.it

Stephanie Schorge s.schorge@ucl.ac.uk

Abstract

Epilepsy is a major health burden, calling for new mechanistic and therapeutic insights. CRISPR–mediated gene editing shows promise to cure genetic pathologies, although hitherto it has mostly been applied *ex-vivo*. Its translational potential for treating non-genetic pathologies is still unexplored. Furthermore, neurological diseases represent an important challenge for the application of CRISPR, because of the need in many cases to manipulate gene function of neurons *in situ*. A variant of CRISPR, CRISPRa, offers the possibility to modulate the expression of endogenous genes by directly targeting their promoters. We asked if this strategy can be effective to treat acquired focal epilepsy. We applied a doxycycline-inducible CRISPRa technology to increase the expression of the potassium channel gene *Kcna1* (encoding Kv1.1) in mouse hippocampal excitatory neurons. CRISPRa-mediated Kv1.1 upregulation led to a substantial decrease in neuronal excitability. Continuous video-EEG telemetry showed that AAV9-mediated delivery of CRISPRa, upon doxycycline administration, decreased spontaneous generalized tonic-clonic seizures in a model of temporal lobe epilepsy. The focal treatment minimizes concerns about off-targets effects in other organs and brain areas. This study provides the proof of principle for a translational CRISPR-based approach to treat neurological diseases characterized by abnormal circuit excitability.

Introduction

Epilepsy affects up to 1% of the population, and 30% of patients continue to experience seizures despite optimal medication (*1, 2*). Although the majority of drug-resistant epilepsies are focal, targeting drugs to a restricted brain region presents major challenges, and potentially curative surgery is limited to a minority of cases where the seizure focus is remote from eloquent cortex (*3*). Gene therapy holds promise as a rational replacement for surgery for intractable pharmaco-resistant epilepsy, and could in principle improve the prospect for seizure freedom in many people (*3, 4*). Several approaches have been proposed to interfere with epileptogenesis or to decrease seizure frequency in chronic epilepsy (*5*). Current experimental gene therapies mainly rely on viral vector-mediated expression of genes encoding normal CNS proteins or exogenous non-mammalian proteins (*4, 6-9*). This approach has several potential limitations, including a finite packaging capacity of viral vectors, difficulty in ensuring normal splicing and post-transcriptional processing, and, in the case of non-mammalian proteins, concerns about immunogenicity. Modulating the expression of endogenous genes, in contrast, would represent an important step toward safe and rational treatment of intractable epilepsy and other neurological diseases.

The DNA editor/regulator CRISPR/Cas9 (*10-12*) represents a powerful tool to modify endogenous genes, not only in somatic cells but also in mammalian neurons (*13, 14*). In addition to permanently altering endogenous gene sequences, CRISPR/Cas can regulate the activity of genes through promoter modulation, an approach known as CRISPR activation (CRISPRa) (*10, 15*). CRISPRa is therefore a promising tuneable tool to increase the expression of genes encoding, for instance, ion channels, in chronic epilepsy in order to restore physiological levels of network activity (*6, 16*). The CRISPRa system is composed by a nuclease-defective Cas9 (dCas9) fused to a transcription activator and a small guide RNA (sgRNA) that targets dCas9 to the promoter of the gene of interest (*10*). The advantages of this system are multiple. First, it is versatile because the targeted gene can be switched simply by changing the sgRNA. Second, CRISPRa preserves the full range of native splice

variants and protein biogenesis mechanisms (*15*). Third, CRISPRa is, in principle, safe because it only alters the promoter activity of genes that are already transcribed in targeted neurons. It can be targeted to specific neurons in the epileptic focus using established viral vectors (*17*).

Here, we report the use of CRISPRa to treat a mouse model of temporal lobe epilepsy, from *in vitro* validation to demonstration of efficacy in reducing seizure frequency *in vivo*.

Results

A CRISPRa system targeting the Kcna1 promoter region increases Kv1.1 expression and decreases neuronal excitability

We first asked if CRISPRa can be exploited to increase endogenous gene expression in glutamatergic neurons and decrease their excitability. As a proof of principle, we chose the *Kcna1* gene. Lentivirus-mediated overexpression of *Kcna1* reduces neuronal excitability and, when targeted to principal cells, suppresses seizures in neocortical models of epilepsy (*6, 18*). We first conducted a bioinformatic analysis to identify its promoter region**.** Alignment of datasets of gene expression and epigenetic markers of actively transcribed genes in perinatal and adult mouse brain identified peaks of enrichment for RNA PolII, mono- and tri-methylation of lys4 and acetylation of lys27 of H3 histone along the gene (Supplementary Figure 1A). One of these regions was located immediately upstream to the annotated *Kcna1* transcription start site (TSS) and identified as a suitable target for CRISPRa. We submitted 200 bps from this region to the *CRISPOR* web tool (*http://crispor.tefor.net*) for sgRNA design, and selected four candidate guides (sg4, sg14, sg19 and sg30) for validation, initially in the P19 cell line. sgRNAs were lipofected individually or in combinations, together with a construct carrying dCas9 fused to the transcriptional activator VP160 (dCas9-VP160) and a Puromycin resistance cassette. dCas9 with sg4, sg14 or sg19, but not with sg30, significantly upregulated the expression of the *Kcna1* gene. We focused on sg4 and sg19,

which induced the highest levels of *Kcna1* expression (Supplementary Figure 1B). When tested in combination, sg4 and sg19 together were also efficacious, but not sg4 and sg30 (Supplementary Figure 1C). We confirmed that the highest efficiency of upregulation of *Kcna1* in primary neurons was achieved with sg19 (Figure 1 B). Consequently, we generated a construct carrying dCAS9-VP160 driven by the Ef1α promoter and either the sg19 targeting the *Kcna1* promoter (Kcna1-dCAS9A) or a control sgRNA targeting LacZ (Ctrl-dCAS9A). Western Blot analysis confirmed increased Kv1.1 protein levels in sg19-treated neurons when compared to the sgLacZ control. Importantly, we detected increased levels of glycosylated Kv1.1, corresponding to mature protein, implying normal processing of the upregulated potassium channel (Figure 1C, D).

The *CRISPOR* tool predicted 250 putative off-target genes for sg19, mostly with a low likelihood score. To evaluate the specificity of CRISPRa we performed a gene expression profile analysis in primary neurons treated with Kcna1-dCAS9A and compared this with Ctrl-dCAS9A transduced neurons. No consistent alteration in the transcriptome of sg19 treated neurons was observed, except for a significant increase in *Kcna1* (red dot, Figure 1E). Six out of 250 predicted off-targets for sg19 were located close to promoters of *Mylpf, Efcab4a, Nudcd2, Pde4b, Gc* and *Vps16* genes. However, none of these genes showed a significant change in expression in either the transcriptome analysis (green dot, Figure 1E) or in quantitative RT-PCR assays (Figure 1F).

Exogenous *Kcna1* overexpression results in a decrease in neuronal excitability (*6*). To test the efficiency of the CRISPRa system, primary neurons were transduced at 1DIV with a lentivirus expressing Kcna1-dCAS9A or Ctrl-dCAS9A. After 14-16DIV we used whole-cell patch clamp recordings to analyse neuronal excitability of both experimental groups (Figure 1G). The maximal firing frequency was significantly decreased in neurons transduced with Kcna1-dCAS9A when compared to Ctrl-dCAS9A (Figure 1H). Other excitability parameters sensitive to Kv1.1 were also changed in neurons transduced with Kcna1-dCAS9A in comparison with Ctrl-dCAS9A: the current threshold was increased, and action potential

width was decreased (Figure 1I). Passive membrane properties and other AP properties were however unchanged (Supplementary Figure 2).

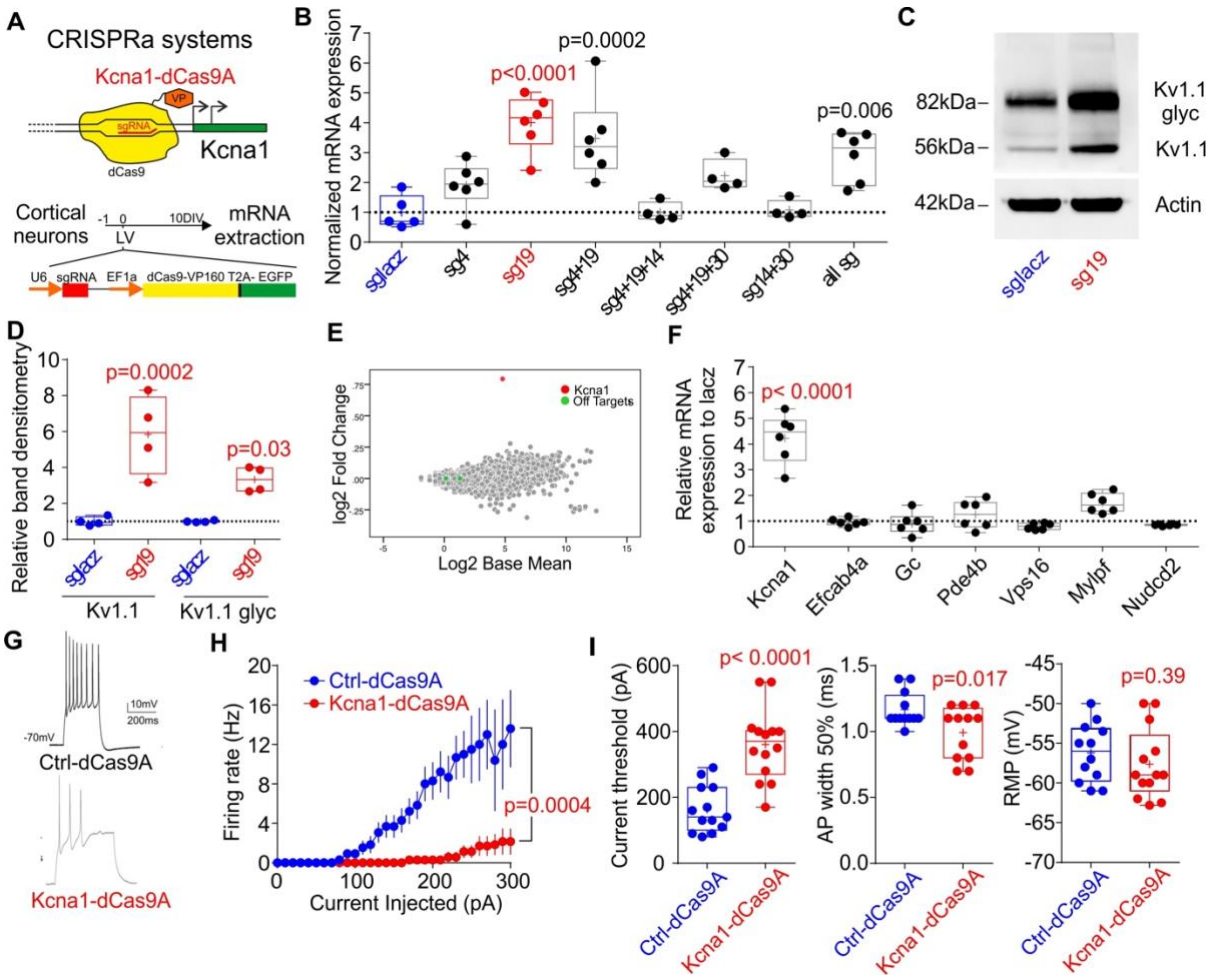

Figure 1: CRISPRa increases endogenous *Kcna1* expression reducing neuronal excitability *in vitro*. A. Schematic representation of the CRISPRa approach to increasing *Kcna1* **B.** *Kcna1* mRNA expression normalised to the control LacZ sgRNA (blue) for the best sgRNAs and combination of different sgRNAs tested in P19 cells (Suppl. Figure 1). One-way ANOVA followed by Bonferroni multi-comparison test vs sgLacZ. **C-D.** Western blot was used to determine Kv1.1 and glycosylated Kv1.1 (glyc) increase in neurons transduce either with dCAS9A and sg19 (red), or sgLacZ (blue). Student's t test. **E.** MA plots showing log2 Fold change as a function of log2 base mean expression of *Kcna1*-dCas9A treated neurons with respect to Ctrl-dCas9A. *Kcna1*, red dot; off-targets, green dots; all other genes, gray dots. **F.** mRNA expression relative to sgLacZ for each off target. The expression level of sgLacZ is represented as the dashed line at 1. Multiple Student's t tests, each compared to control and corrected for multiple comparison (α= 0.0083). **G.** Representative patch clamp traces of neurons

transduced either with Ctrl-dCAS9A (sgLacZ, blue) or Kcna1-dCAS9A (sg19, red) and injected with 300pA steps in current clamp. **H.** Firing rate in response to different current injections for neurons transduced with ctrl-dCAS9A or Kcna1-dCAS9A. Two-way RM ANOVA. **I.** Neuronal and action potential (AP) properties in neurons transduced with ctrl-dCAS9A or Kcna1-dCAS9A. Student's t test.

Kcna1-dCas9A decreases CA1 pyramidal cell excitability

In order to test the efficacy of CRISPRa *in vivo*, we subcloned the CRISPRa elements in two separate AAV9 vectors. One AAV vector carried the dCAS9-VP64 under the control of a rtTA responsive element (TRE), while the other vector included sg19 (or sgLacZ as a control) element and a human Synapsin promoter (hSyn) upstream to a floxed rtTA-t2a-tdTomato cassette. This experimental design allowed the Kcna1-dCas9A system to be activated in forebrain excitatory neurons of Camk2a-cre mice transduced with both AAVs, but only after doxycycline administration (Figure 2A, B). We co-injected both AAVs in the hippocampus of 2-3 month old Camk2a-CRE mice, which were subsequently fed with a doxycycline diet for 3 weeks and then sacrificed for preparation of acute brain slices. Pyramidal neurons in the CA1-subiculum of the ventral hippocampus were recorded with whole-cell patch clamp to measure their excitability (Figure 2B, C and Supplementary Figure 3, 4). Consistent with data from primary cultures, neurons transduced with Kcna1-dCAS9A showed a decreased firing rate and increased current threshold when compared with Ctrl-dCAS9A expressing neurons (Figure 2 E). A minor difference from primary cortical cultures was that the half width of the first spike was not significantly different between Kcna1-dCAS9A and Ctrl-dCAS9A expressing neurons (Figure 1 I). However, a significant decrease was seen when all the APs during the current step protocol were pooled (Figure 2 F). Finally, we applied activity clamp, a method to assess neuronal excitability in the face of epileptiform barrages of excitation (*19*). Neurons expressing Kcna1-dCAS9A fired less than neurons expressing Ctrl-dCAS9A when exposed to the same simulated synaptic input. Taken

together, these results support using Kcna1-dCAS9A as a candidate antiepileptic gene therapy (Figure 2 G).

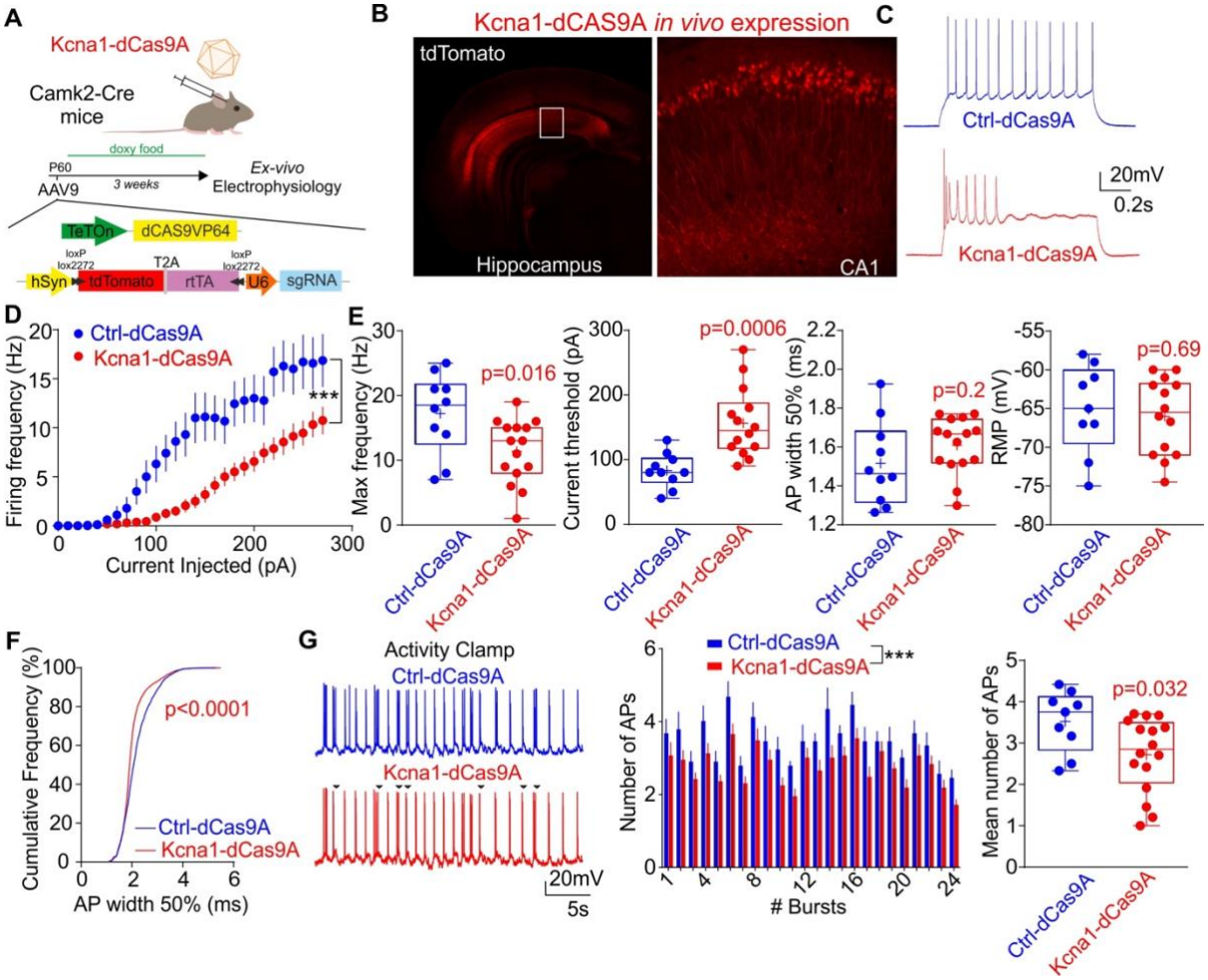

Figure 2: CRISPRa delivered with AAV9 increases endogenous *Kcna1* expression and reduces CA1 pyramidal neuron excitability A. Schematic representation of the approach for *ex vivo* quantification of CRISPRa effects. **B.** Representative live image of *Kcna1*-dCAS9A expression in the hippocampus (inset= CA1 region, Red= tdTomato) **C.** Representative patch clamp traces of CA1 pyramidal neurons, transduced either with Ctrl-dCAS9A (sgLacZ, blue) or Kcna1-dCAS9A (sg19, red) in pryramidal neurons injected with 280pA steps in current clamp. **D.** Firing rate in response to different current steps for neurons transduced with Ctrl-dCAS9A or Kcna1-dCAS9A. Two-way RM ANOVA. **E.** Neuronal and action potential (AP) properties in neurons transduced with Ctrl-dCAS9A or Kcna1-dCAS9A. Maximal firing rate, current threshold to elicit the first AP, AP width and resting membrane potential are shown. Student's t test. **F.** Cumulative frequency (%) of the AP widths in

neurons injected with 280pA of current. Kolmogorov-Smirnov test for cumulative distributions. **G.** Activity clamp protocol to mimic 24 interictal bursts of synaptic input from an epileptic network in neurons transduced with Ctrl-dCAS9A or Kcna1-dCAS9A (*left*). Black arrows represent the APs missed in the Kcna1-dCAS9A neurons. Number of APs for each burst showed as mean ± sem (*middle*). Two-way ANOVA. The histogram represents the average number of APs for each neuron in the 24 bursts (*right*). Student's t test.

Kcna1-dCas9A decreases seizure frequency in a mouse model of temporal lobe epilepsy

We administered Kcna1-dCAS9A in a mouse model of acquired epilepsy. C57BL/6J WT animals were injected with kainic acid (KA) in the right amygdala (*20*). This induced a period of status epilepticus (SE), which was quantified by video recording to monitor seizure severity (Supplementary Figure 5 and Video 1). One week later, we injected either Kcna1-dCAS9A or Ctrl-dCAS9A AAVs in the right ventral hippocampus, and at the same time we implanted wireless EEG transmitters (bandwidth 1-256 Hz). For these experiments an AAV9 carrying a non-floxed rtTA-t2a-tdTomato cassette and driven by a Camk2a promoter was delivered to provide specific expression in excitatory neurons. After a week of recovery to allow expression of the constructs, we started continuous video-EEG recording for 2 weeks (baseline) and then continued recording for 2 further weeks with doxycycline administration (Figure 3A). Immunohistochemistry of the injected hippocampi showed expression of the tdTomato reporter in dentate gyrus granule cells and hippocampal CA3 excitatory neurons, as well as CA1 pyramidal cells (Figure 3B, Supplementary Figure 6). We extracted both the ipsilateral and contralateral hippocampi of 11 mice after the EEG recordings to analyse *Kcna1* and dCas9 expression. Two hippocampi failed to express dCas9 and were excluded from the analysis. The other 9 hippocampi (5 Ctrl-dCAS9A and 4 Kcna1-dCAS9A) expressed dCAS9 and showed a 50% increase in *Kcna1* expression in mice transduced with Kcna1-dCAS9A compared to Ctrl-dCAS9A (Figure 3C). To investigate the efficiency of Kcna1-dCAS9 to treat chronic temporal lobe epilepsy we analysed the frequency of

generalized tonic-clonic seizures (Racine stage 5) in each animal before and after doxycycline administration (Figure 3D-F; Supplementary Figure 7; Video 2). Animals treated with Kcna1-dCAS9A showed a significant reduction of the number of seizures after doxycycline was added to the food (Figure 3 D-F). Other EEG parameters such as broadband power and seizure duration were unchanged (Supplementary Figure 5 E). Taken together, these results suggest that Kcna1-dCAS9A increases the threshold for triggering a generalized tonic-clinic seizure but otherwise does not change general network properties.

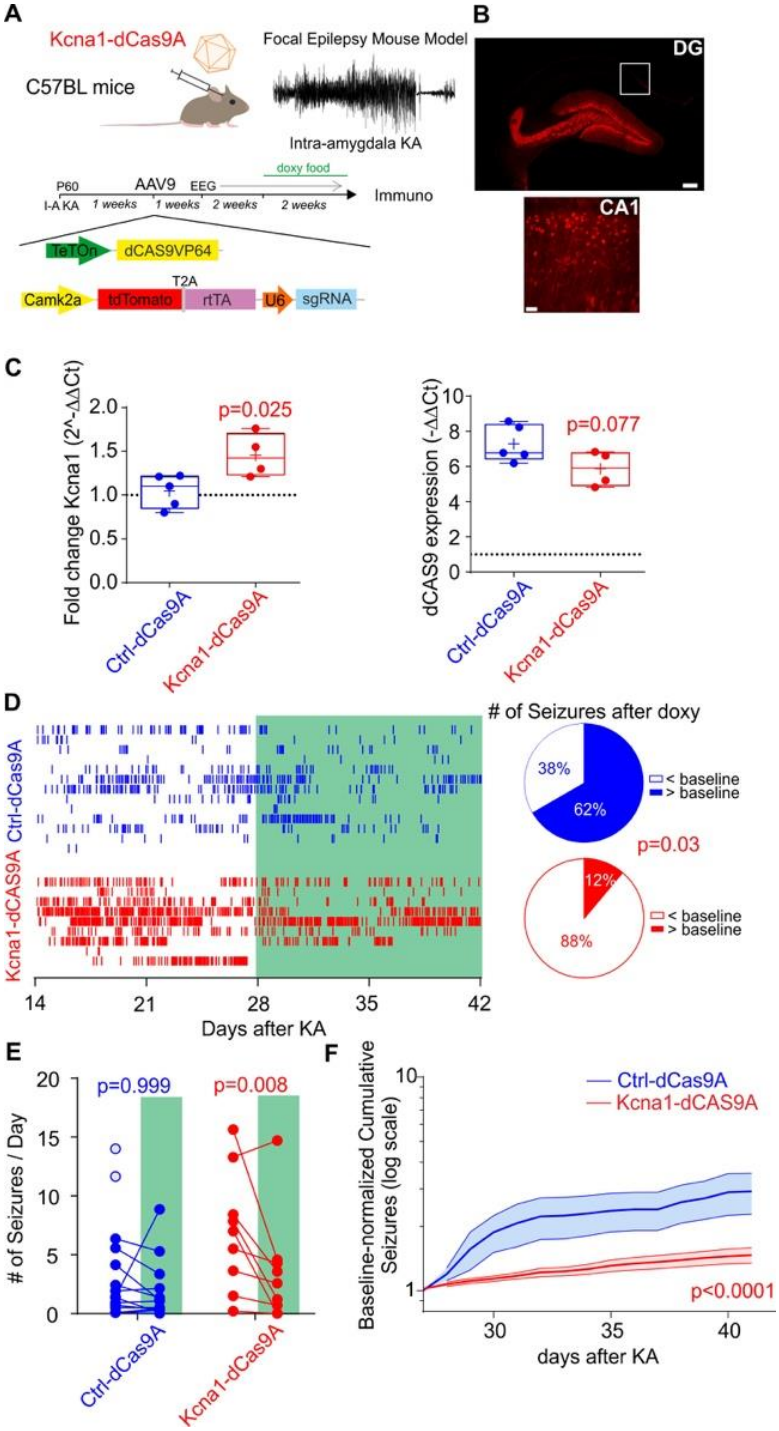

Figure 3: CRISPRa-Kcna1 decreases number of seizures in a mouse model of acquired intractable temporal lobe epilepsy. A. Schematic representation of the CRISPRa approach used *in vivo* to treat the intra-amygdala kainic acid focal model of temporal lobe epilepsy. **B.** Representative immunofluorescence 7 weeks after status epilepticus (SE) of neurons transduced with Ctrl-dCAS9A 4 weeks after SE. Scale bar DG: 250μm; CA1:50 μm. **C.** Kcna1 and dCAS9 expression in the ipsilateral normalized to the contralateral hippocampus in

epileptic mice transduced with either Ctrl-dCAS9A or Kcna1-dCAS9A at the end of the experiments. Student's t test **D.** *Left.* Scatter plot of seizure number before and after doxycycline administration. *Right.* Pie charts of the changes in number of seizures in doxycycline food compared to the baseline. Fisher's exact test. At 4 weeks the food was changed to doxycycline diet to induce expression of dCAS9a. **E.** Histogram of the number of seizures/day before and after doxycycline administration in control-dCAS9 and Kcna1-dCAS9 treated animals. Two-way ANOVA followed by Bonferroni multi-comparison test. **F.** Cumulative plot of seizures normalised to the baseline in mice transduced with either ctrl-dCAS9A or Kcna1-dCAS9A. Two-way ANOVA.

Discussion

Although CRISPR has attracted intense interest as a possible treatment for inherited or acquired genetic disorders, it has, hitherto, received much less attention as a potential tool to treat acquired non-genetic diseases. The overwhelming majority of epilepsy cases, which represent an enormous disease burden, are not thought to be due to single gene mutations but are acquired during life, often secondary to a variety of brain insults such as infections, strokes and injuries (*1, 2*). Here we have shown that CRISPRa can be used to increase endogenous *Kcna1* expression to modulate neuronal activity, and thereby decrease the frequency of seizures in a mouse model of chronic temporal lobe epilepsy. This approach can potentially be used to regulate the expression of any gene, opening the way to treating many other neurological diseases associated with altered transcription. At present the main obstacles to translation for the CRISPR/Cas9 toolbox are absence of long-term data on potential immunogenicity of the bacterial nuclease in humans and possible off-targets that have not been detected by transcriptomic analysis (*21*). CRISPRa is, in principle, less likely to have deleterious off-target effects than gene editing because it does not cleave DNA (*17, 22*), but further research is necessary.

Among distinct advantages of CRISPRa over exogenous gene delivery is the possibility to select one or more sgRNAs to tailor the exact level of gene expression independently by the number of viral copies effectively entered within each neuron. In addition, several sgRNAs can be designed to control the transcription of heteromultimeric proteins such as $GABA_A$ or NMDA receptors, or multiple genes in a signaling pathway. Finally, if gene supplementation therapy is strongly biased by the overall gene size which should not exceed the viral capacity cargo, the CRISPRa can be potentially applied to control the activity of any gene irrespective of its length (*23*). Although the present study made use of two AAVs to allow inducible activation of CRISPRa and expression of a fluorescent reporter protein, for clinical translation these features would not be required, and so it should be possible to package both the dCAS9 and the sgRNA in a single AAV to simplify clinical delivery. Further refinements can be considered, such as the use of an inducible promoter to allow the

therapy to be switched off (*16*), which would not be possible with a gene editing strategy. These results demonstrate that CRISPR-mediated control of gene expression can be successfully exploited to modulate neuronal activity to obtain a significant and long-term clinical management of chronic seizures in an experimental model of intractable temporal lobe epilepsy.

Materials and Methods

Study Design

This study aimed to test the hypothesis that upregulating endogenous genes (e.g. *Kcna1*) with CRISPRa can treat chemoconvulsant-induced temporal lobe epilepsy. The experiments were designed to achieve a power >0.8 with an α = 0.05. For *in vivo* experiments the 3Rs guidelines for animal welfare were also followed. Outliers were not excluded and at least 3 independent repetitions were performed. Exclusion criteria were applied for all the recordings (see methods below). All the experiments were randomized and researchers were blinded during recordings and analysis.

Animals and ethics.

All experimental procedures were carried out in accordance with the UK Animals (Scientific Procedures) Act 1986. C57BL/6J and Camk2a-CRE mice were used for the experiments.

Plasmids. sgRNAs were cloned in a lentiviral pU6 vector. Ef1alpha-dCas9VP160-T2A-PuroR, was derived from pAC94-pmax-dCas9VP160-2A-puro, a gift of R. Jaenisch (Addgene plasmid # 48226). The dCas9VP160-2A-puro cassette was subcloned in a TetO-FUW vector and then restriction digested with HpaI/AfeI and blunt cloned into an Ef1alpha-GFP vector after GFP removal by SmaI/EcoRV digestion. Ef1alpha-dCas9VP160-T2A-GFP was obtained by restriction digestion of Ef1alpha-dCas9VP160-T2A-Puro^R with AscI/XbaI that removed VP160-T2A-PuroR; the VP160-T2A fragment was then obtained by AscI/XhoI digestion from Ef1alpha-dCas9VP160-T2A-Puro^R while GFP fragment was PCR amplified with primers containing XhoI/XbaI restritction sites; finally, the two fragments were ligated together into the vector. To obtain a single vector containing both dCas9A and sgRNA, the pU6-sgRNA cassette was HpaI digested and cloned into Ef1alpha-dCas9VP160. AAV-TRE-dCas9-VP64 was obtained by restriction digestion of AAV-SpCas9 (gift of F. Zhang, Addgene # PX551) where the Mecp2 promoter was removed by XbaI/AgeI digestion and TRE promoter was amplified with the following primers: FWXbaI:

GCTCTAGACCAGTTTGGTTAGATCTC and RV AgeI GCACCGGTGCGATCTGACGGTTCACT. SpCas9 was removed with AgeI/EcoRI and Cas9m4-VP64 (gift of G. Church, addgene # 47319) was digested with AgeI/EcoRI. The VP64 fragment was PCR amplified with following primers with EcoRI sites: F: GATCATCGAGCAAATAAGCGAATTCTC and R: gctaaGAATTCTTA-TCTAGAGTTAATCAGCATG. The AAV vector containing the sgRNA cassette was derived from pAAV-U6sgRNA (SapI)_hSyn-GFP-KASH-bGH (PX552 was a gift of F. Zhang, Addgene # 60958): sg19 or lacZ where cloned under U6 promoter and the GFP was removed by KpnI/ClaI digestion and replaced by a DIO-rtTA-T2A-Tomato cassette. This vector was used for the work in Camk2a-Cre mice. For the work in C57/Bl6 mice, this vector was XbaI/ClaI-digested to remove both hSyn promoter, and the DIO-rtTA-T2A-Tomato cassette was replaced by a Camk2a promoter amplified with NheI-KpnI and a tTA T2a tomato cassette amplified with KpnI ClaI, ligated together in the vector.

Virus preparation. Lentiviruses were produced as previously described with a titer of 10^7-10^8 IU/ml (*24*). AAVs were produced as previously described with a titer higher than 10^12 vg/ml (*25*). The TRE-dCas9-VP64 AAV was produced by VectorBuilder with a titer of 8 x 10^12 vg/ml.

P19 cell line. P19 cells were cultured in alpha-MEM (Sigma-Aldrich) supplemented fetal bovine serum non-essential amino acids, sodium pyruvate, glutamine and penicillin/streptomycin and split every 2-3days using 0.25% trypsin. For transfection, Lipofectamine 3000 (Thermo Fisher Scientific) was used according to the manufacturer's instructions.

Primary neuronal culture and lentivirus transduction. Cortical neurons were isolated from P0 C57Bl/6J mouse pups as previously described (*26*) and at 1 DIV were transduced with lentiviruses. qRT-PCR, RNA seq, Western blot analysis and electrophysiology recordings were performed 14-16 days after transduction.

RNA isolation and quantitative RT- PCR. RNA was extracted using TRI Reagent (Sigma) according to the manufacturer's instructions. For quantitative RT-PCR (RT-qPCR), cDNA synthesis was obtained using the ImProm-II Reverse Transcription System (Promega) and RT-qPCR were performed with custom designed oligos (Table 1) using the Titan HotTaq EvaGreen qPCR Mix (BIOATLAS). Analysis of relative expression was performed using the $\Delta\Delta C_T$ method, relative to Ctrl-dCas9A condition. To determine Kcna1 expression in vivo, $\Delta\Delta C_T$ was determined in Ctrl- dCas9A or in Kcna1-dCas9A injected hippocampi relative to contralateral hippocampi in epileptic animals at the end of the recordings.

Western Blot. Total neuronal protein extracts were obtained from the lysis of primary neurons by RIPA lysis buffer (150 mM NaCl, 1% Triton, 0.5% sodium deoxycholate, 0.1% sodium dodecyl sulfate, Tris pH 8.0 50 mM, protease inhibitor cocktail) two weeks after infection with the CRISPRa-Kcna1 system. Lysates were kept on ice for 30 minutes by vortexing every 10 minutes and then centrifuged at 4° C for 5 minutes at 5000 rpm. Supernatants with solubilized proteins were collected in new tubes and stored at -80° C until use. Western blot analysis was performed using primary antibodies against the following proteins: anti-Kv1.1 (1:1000, Neuromab) anti- α/βActin (1:10000, Sigma).

Bioinformatic analysis. Encyclopedia of DNA Elements (ENCODE) and the Functional ANnoTation Of the Mammalian genome (FANTOM) (*27*) databases were used to download transcriptomics and epigenetics NGS data. Tracks were visualized along the mm10 mouse reference genome with the Integrative Genome Viewer (IGV) (*28*).

Off-targets. Employing the free Galaxy web-tool (https://usegalaxy.org/) we generated two datasets: one containing sg19 off-target sequences predicted by *CRISPOR* web tool (*http://crispor.tefor.net*) and one containing all the 500 bp genomic regions (NCBI37/mm9) upstream to transcription start sites (TSS) of annotated transcripts. Intersecting the two datasets, all sg19 off-target sequences in putative gene promoters were derived. To identify genes regulated by putative promoters, the sequence of the predicted off-targets was aligned

by IGV to the reference genome and to transcripts annotated in ENSEMBL database. Validation of expression levels of putative off-target genes was performed by RT-qPCR.

RNA-seq. RNA libraries were generated starting from 1 ug of total RNA extracted from sglacz- and sg19-dCAS9A neurons at 10 DIV. RNA quality was assessed by using a Tape Station instrument (Agilent) and only RNA samples with Integrity Number (RIN) ≥ 8 were analyzed. RNA was processed according to the Lexogen QuantSeq 3' mRNA-Seq Library Prep Kit protocol and the libraries were sequenced on an Illumina NextSeq 500 with 75bp stranded reads. Illumina Real Time Analysis Software was employed for image processing. Fastq files were aligned to the mouse genome (NCBI37/mm9) with Bowtie2. Differential gene expression and functional enrichment analyses were performed with DESeq2 and GSEA, respectively. SPSS (IBM) and R statistical packages were employed for Statistical analysis.

Slice preparation. Camk2a-CRE mice of either sex (2-3 months old) were killed by cervical dislocation under isoflurane. Brains were quickly dissected into ice cold oxygenated slicing solution (in mM: 75 sucrose, 2.5 KCl, 25 $NaHCO_3$, 25 glucose, 7 $MgCl_2$, 0.5 $CaCl_2$) and cut into 300 µm coronal slices using a Leica VT1200S vibratome (Leica). Slices were stored submerged in oxygenated recording artificial cerebrospinal fluid (aCSF) (in mM: 25 glucose, 125 NaCl, 2.5 KCl, 25 $NaHCO_3$, 1 $MgCl_2$, 1.25 $NaH_2PO_4.H_2O$ and 2 $CaCl_2$) at 32°C for 30min and at room temperature for a further 30min before recording.

Electrophysiology. *In vitro.* For current-clamp recordings, the internal solution contained (in mM): 126 K-gluconate, 4 NaCl, 1 MgSO4, 0.02 CaCl2, 0.1 BAPTA, 15 Glucose, 5 HEPES, 3 ATP-Na2, 0.1 GTP-Na, pH 7.3. The extracellular (bath) solution contained (in mM): 2 CaCl2, 140 NaCl, 1 MgCl2, 10 HEPES, 4 KCl, 10 glucose, pH 7.3. D-(−)-2-amino-5-phosphonopentanoic acid (D-AP5; 50 µM), 6-cyano-7-nitroquinoxaline-2,3-dione (CNQX; 10 µM) and picrotoxin (PTX; 30 µM) were added to block synaptic transmission. Transduced excitatory neurons were identified with EGFP fluorescence and from a pyramidal somatic shape. Neurons with unstable resting potential (or > -50mV), access resistance (R_a) > 15 MΩ and/or holding current >200 pA at -70mV were discarded. Bridge balance compensation was

applied and the resting membrane potential was held at -70 mV. A current step protocol was used to evoke action potentials (APs), by injecting 250 ms long depolarizing current steps of increasing amplitude from -20pA (Δ 10pA). Recordings were acquired using a Multiclamp 700A amplifier (Axon Instruments, Molecular Devices) and a Power3 1401 (CED) interface combined with Signal software (CED), filtered at 10 kHz and digitized at 50 kHz.

Ex-vivo current clamp recordings. Current clamp recordings were performed in standard external solution in the presence of DL-AP5 (50 μM), 6-cyano-7-nitroquinoxaline-2,3-dione (CNQX; 10 μM) and PTX (30 μM) to block NMDA, AMPA/kainate, and $GABA_A$ receptors, respectively. The internal solution was the same as for in vitro patch clamp recordings. Neurons with holding current >100 pA and R_a >20 MΩ upon whole-cell break-in in voltage clamp mode and membrane potential less negative than -60mV in current clamp were not considered for analysis. A 1440 Digidata (Molecular Devices) or Power3 1401 (CED) interface and Multiclamp 700A (Molecular Devices) amplifier were used.

In vitro and ex-vivo electrophysiology analysis. All the electrophysiology analysis was performed with an automated Python script. Passive properties were calculated from the hyperpolarizing steps of the current clamp steps protocol. Input resistance was averaged from three current steps (2 negative and one positive). Capacitance was calculated from the hyperpolarizing current step as follows. Firstly, the input resistance was determined as the steady-state $\Delta V/\Delta I$ (voltage/current), then the cell time constant (tau) was obtained by fitting the voltage relaxation between the baseline and the hyperpolarizing plateau. Capacitance was then calculated as tau/resistance. Single action potential parameters were calculated as previously described (*29*). An event was detected as an action potential if it crossed 0mV and if the rising slope was >20mV/ms in a range of injected currents from 0pA to 500pA. All the experiments were performed at room temperature (22-24°C). All recordings and analysis were carried out blind to vector transduced.

Activity clamp. The template simulating the barrage of synaptic conductances during epileptiform bursts was previously described (*19*). Dynamic clamp software (Signal 6.0,

Cambridge Electronic Design, Cambridge, UK) and a Power3 1401 (CED) were used to inject both excitatory and inhibitory conductance templates simultaneously in a neuron recorded in current clamp configuration (iteration frequency 15 kHz). E_{rev} was set to 0 mV and -75 mV for excitatory and inhibitory conductances respectively, and corrected for a liquid junction potential of 14.9 mV. Incrementing synaptic conductances were injected in recorded neurons to establish the conductance threshold for action potential generation. Current clamp recordings for activity clamp were performed with the same external and internal solutions as given above.

Surgical procedures. All the surgery procedures were performed in adult mice (2-3 months) anesthetized and placed in a stereotaxic frame (Kopf).

Epileptic model. 0.3μg of 10mg/ml kainic acid (Tocris) was injected in a volume of in 200nl in the right amygdala (AP: -0.94; ML: 2.85; DV: 3.75) at 200nl/min under isoflurane anaesthesia (surgery time 10-15 minutes). The mice were allowed to recover from anaesthesia at 32°C for 5 minutes and then moved back to their cage where they were monitored closely during status epilepticus (SE). SE usually started 10-15 minutes after complete recovery and always stopped 40 minutes after KA injection with 10mg/Kg intraperitoneal diazepam.

Stereotaxic viral injection. 300nl of AAV9 viruses (1:1) were injected with a 5μl Hamilton syringe (33 gauge) at 100nl/min in 3 different coordinates of the right ventral hippocampus (Antero-Posterior: -2/3 bregma/lamda distance; Medio-Lateral: -3; Dorso-Ventral: 3.5/3/2.5). the needle was kept in place for 10 minutes after each injection.

Transmitter implantation. An electrocorticogram (ECoG) transmitter (A3028C-CC Open Source Instruments, Inc) was subcutaneously implanted and the recording electrode was placed above the viral injection site (Antero-Posterior: -2/3 bregma/lamda distance; Medio-Lateral: -3). The ground electrode was placed in the contralateral frontal hemisphere.

Exclusion criteria. Only animals recorded for the entire period of the experiment (6 weeks after KA) were used in the analysis. At the end of the experiments some animal tissues were analysed with qRT-PCR and others were verified with immunofluorescence. On total of 42 mice injected with kainic acid, 34 animals (80%) were implanted and injected. 24 were recorded for entire duration of the experiment. 2 did not express dCAS9 and for this reason were excluded from the analysis. 22 mice were used for the analysis (13 Ctrl-dCAS9A and 9 Kcna1-dCAs9A).

EEG (or ECoG) recordings. The ECoG was acquired wirelessly using hardware and software from Open Source Instruments, Inc. The ECoG was sampled at a frequency of 256Hz, band-pass filtered between 1 and 160Hz, and recorded continuously for the duration of the experiments. The animals were housed independently in a Faraday cage.

EEG analysis. Spontaneous seizures were detected from chronic recordings using a semi-automated supervised learning approach (suppl. figure 7). First, a library containing examples of epileptiform activity was built using seizures identified from visual inspection of ECoG data. The recordings were saved in hour-long files, and for each seizure this full hour was included in the library. Recordings were chunked into 5 second blocks that were labelled as either “ictal” or “interictal” if they contained epileptiform-labelled activity or not, respectively. For each five second chunk of recording, 15 features were extracted (suppl. figure 7 and see online resource below). A random forest discriminative classifier was trained on the features and labels of each of the 5 second examples in the library (*30*). In addition, cross validation generated classifier predictions were used to parameterise a Hidden Markov Model in which the hidden states were the human annotations and the emissions the classifier predictions. For automated detection of epileptiform activity from unlabelled recordings, the discriminative classifier was first used to predict the class of consecutive five second chunks. We then applied the forward-backward algorithm to obtain the marginal probability of being in seizure state for each recording chunk given the surrounding classifier predictions. The smoothed predictions were then manually verified,

false positives removed from the analysis and start and end locations adjusted. In order to quantify the performance of our approach, we randomly selected four 2 week chunks of recordings and visually examined the traces for seizures and compared to classifier predictions (blinded). During the 8 weeks, we did not detect visually any seizures that were not marked by the classifier – as such, for this model of epilepsy, our false negative rate was less than 1/300. False positives were less of a concern, but in general we observed << n seizures for a given period of time. For further information and code, please see: https://github.com/jcornford/pyecog.

Video recordings. IP cameras from Microseven (https://www.microseven.com/index.html) were used and synchronised via the Windows time server to the same machine as the ECoG was acquired. Continuous video recordings produced 6 videos/hour.

Immunohistochemistry. Immunostaining was performed on 50µm mice brain sections with the following antibodies: mouse anti-GAD67 (MAB5406, Merck), rabbit anti-RFP (600-401-379, Rockland), Alexa Fluor 555 goat anti-rabbit (A32732, Invitrogen) and Alexa Fluor 488 goat anti-mouse (A32723, Invitrogen). Images were acquired with ZEN software (Zeiss) on a LSM710 confocal microscope (Zeiss) and co-localization analysis of tdTomato and GAD67 were performed with ImageJ 1.51n (Wayne Rasband, National Institute of Health) plugin 'JACoP'.

Statistics. Data are plotted as box and whiskers, representing interquartile range (box), median (horizontal line), and max and min (whiskers), together with all the points. The mean is further shown as "+". The statistical analysis performed is shown in each figure legend. Deviation from normal distributions was assessed using D'Agostino-Pearson's test, and the F-test was used to compare variances between two sample groups. Student's two-tailed *t*-test (parametric) or the Mann-Whitney test (non-parametric) were used as appropriate to compare means and medians. Fisher's exact test was used to analyze the contingency table. To compare two groups at different time points we used two-way repeated measure ANOVA, followed by Bonferroni post-hoc test for functional analysis. Statistical analysis was

carried out using Prism (GraphPad Software, Inc., CA, USA) and SPSS (IBM SPSS statistics, NY, USA).

References

1. P. Kwan, S. C. Schachter, M. J. Brodie, Drug-resistant epilepsy. *N Engl J Med* **365**, 919-926 (2011).
2. F. Tang, A. M. S. Hartz, B. Bauer, Drug-Resistant Epilepsy: Multiple Hypotheses, Few Answers. *Front Neurol* **8**, 301 (2017).
3. D. M. Kullmann, S. Schorge, M. C. Walker, R. C. Wykes, Gene therapy in epilepsy-is it time for clinical trials? *Nat Rev Neurol* **10**, 300-304 (2014).
4. A. Lieb, Y. Qiu, C. L. Dixon, J. P. Heller, M. C. Walker, S. Schorge, D. M. Kullmann, Biochemical autoregulatory gene therapy for focal epilepsy. *Nat Med*, (2018).
5. M. Simonato, Gene therapy for epilepsy. *Epilepsy Behav* **38**, 125-130 (2014).
6. R. C. Wykes, J. H. Heeroma, L. Mantoan, K. Zheng, D. C. MacDonald, K. Deisseroth, K. S. Hashemi, M. C. Walker, S. Schorge, D. M. Kullmann, Optogenetic and potassium channel gene therapy in a rodent model of focal neocortical epilepsy. *Sci Transl Med* **4**, 161ra152 (2012).
7. D. Katzel, E. Nicholson, S. Schorge, M. C. Walker, D. M. Kullmann, Chemical-genetic attenuation of focal neocortical seizures. *Nat Commun* **5**, 3847 (2014).
8. E. Krook-Magnuson, C. Armstrong, M. Oijala, I. Soltesz, On-demand optogenetic control of spontaneous seizures in temporal lobe epilepsy. *Nat Commun* **4**, 1376 (2013).
9. R. C. Wykes, D. M. Kullmann, I. Pavlov, V. Magloire, Optogenetic approaches to treat epilepsy. *J Neurosci Methods* **260**, 215-220 (2016).
10. A. A. Dominguez, W. A. Lim, L. S. Qi, Beyond editing: repurposing CRISPR-Cas9 for precision genome regulation and interrogation. *Nat Rev Mol Cell Biol* **17**, 5-15 (2016).
11. P. D. Hsu, E. S. Lander, F. Zhang, Development and applications of CRISPR-Cas9 for genome engineering. *Cell* **157**, 1262-1278 (2014).
12. M. Adli, The CRISPR tool kit for genome editing and beyond. *Nat Commun* **9**, 1911 (2018).
13. M. Heidenreich, F. Zhang, Applications of CRISPR-Cas systems in neuroscience. *Nat Rev Neurosci* **17**, 36-44 (2016).
14. K. Suzuki, Y. Tsunekawa, R. Hernandez-Benitez, J. Wu, J. Zhu, E. J. Kim, F. Hatanaka, M. Yamamoto, T. Araoka, Z. Li, M. Kurita, T. Hishida, M. Li, E. Aizawa, S. Guo, S. Chen, A. Goebl, R. D. Soligalla, J. Qu, T. Jiang, X. Fu, M. Jafari, C. R. Esteban, W. T. Berggren, J. Lajara, E. Nunez-Delicado, P. Guillen, J. M. Campistol, F. Matsuzaki, G. H. Liu, P. Magistretti, K. Zhang, E. M. Callaway, K. Zhang, J. C. Belmonte, In vivo genome editing via CRISPR/Cas9 mediated homology-independent targeted integration. *Nature* **540**, 144-149 (2016).
15. H. K. Liao, F. Hatanaka, T. Araoka, P. Reddy, M. Z. Wu, Y. Sui, T. Yamauchi, M. Sakurai, D. D. O'Keefe, E. Nunez-Delicado, P. Guillen, J. M. Campistol, C. J. Wu, L. F. Lu, C. R. Esteban, J. C. Izpisua Belmonte, In Vivo Target Gene Activation via CRISPR/Cas9-Mediated Trans-epigenetic Modulation. *Cell* **171**, 1495-1507 e1415 (2017).
16. R. C. Wykes, G. Lignani, Gene therapy and editing: Novel potential treatments for neuronal channelopathies. *Neuropharmacology* **132**, 108-117 (2018).
17. M. F. La Russa, L. S. Qi, The New State of the Art: Cas9 for Gene Activation and Repression. *Mol Cell Biol* **35**, 3800-3809 (2015).
18. A. Snowball, E. Chabrol, R. C. Wykes, A. Lieb, K. Hashemi, D. M. Kullmann, M. Walker, S. Schorge, Epilepsy gene therapy using non-integrating lentiviral delivery of an engineered potassium channel gene. *bioRxiv*, (2018).
19. G. Morris, M. Leite, D. M. Kullmann, I. Pavlov, S. Schorge, G. Lignani, Activity Clamp Provides Insights into Paradoxical Effects of the Anti-Seizure Drug Carbamazepine. *J Neurosci* **37**, 5484-5495 (2017).
20. E. M. Jimenez-Mateos, T. Engel, P. Merino-Serrais, R. C. McKiernan, K. Tanaka, G. Mouri, T. Sano, C. O'Tuathaigh, J. L. Waddington, S. Prenter, N. Delanty, M. A.

Farrell, D. F. O'Brien, R. M. Conroy, R. L. Stallings, J. DeFelipe, D. C. Henshall, Silencing microRNA-134 produces neuroprotective and prolonged seizure-suppressive effects. *Nat Med* **18**, 1087-1094 (2012).
21. M. Kosicki, K. Tomberg, A. Bradley, Repair of double-strand breaks induced by CRISPR-Cas9 leads to large deletions and complex rearrangements. *Nat Biotechnol*, (2018).
22. Y. Zheng, W. Shen, J. Zhang, B. Yang, Y. N. Liu, H. Qi, X. Yu, S. Y. Lu, Y. Chen, Y. Z. Xu, Y. Li, F. H. Gage, S. Mi, J. Yao, CRISPR interference-based specific and efficient gene inactivation in the brain. *Nat Neurosci* **21**, 447-454 (2018).
23. S. Konermann, M. D. Brigham, A. E. Trevino, J. Joung, O. O. Abudayyeh, C. Barcena, P. D. Hsu, N. Habib, J. S. Gootenberg, H. Nishimasu, O. Nureki, F. Zhang, Genome-scale transcriptional activation by an engineered CRISPR-Cas9 complex. *Nature* **517**, 583-588 (2015).
24. G. Colasante, G. Lignani, A. Rubio, L. Medrihan, L. Yekhlef, A. Sessa, L. Massimino, S. G. Giannelli, S. Sacchetti, M. Caiazzo, D. Leo, D. Alexopoulou, M. T. Dell'Anno, E. Ciabatti, M. Orlando, M. Studer, A. Dahl, R. R. Gainetdinov, S. Taverna, F. Benfenati, V. Broccoli, Rapid Conversion of Fibroblasts into Functional Forebrain GABAergic Interneurons by Direct Genetic Reprogramming. *Cell Stem Cell* **17**, 719-734 (2015).
25. G. Morabito, S. G. Giannelli, G. Ordazzo, S. Bido, V. Castoldi, M. Indrigo, T. Cabassi, S. Cattaneo, M. Luoni, C. Cancellieri, A. Sessa, M. Bacigaluppi, S. Taverna, L. Leocani, J. L. Lanciego, V. Broccoli, AAV-PHP.B-Mediated Global-Scale Expression in the Mouse Nervous System Enables GBA1 Gene Therapy for Wide Protection from Synucleinopathy. *Mol Ther* **25**, 2727-2742 (2017).
26. G. M. Beaudoin, 3rd, S. H. Lee, D. Singh, Y. Yuan, Y. G. Ng, L. F. Reichardt, J. Arikkath, Culturing pyramidal neurons from the early postnatal mouse hippocampus and cortex. *Nat Protoc* **7**, 1741-1754 (2012).
27. P. Carninci, A. Sandelin, B. Lenhard, S. Katayama, K. Shimokawa, J. Ponjavic, C. A. Semple, M. S. Taylor, P. G. Engstrom, M. C. Frith, A. R. Forrest, W. B. Alkema, S. L. Tan, C. Plessy, R. Kodzius, T. Ravasi, T. Kasukawa, S. Fukuda, M. Kanamori-Katayama, Y. Kitazume, H. Kawaji, C. Kai, M. Nakamura, H. Konno, K. Nakano, S. Mottagui-Tabar, P. Arner, A. Chesi, S. Gustincich, F. Persichetti, H. Suzuki, S. M. Grimmond, C. A. Wells, V. Orlando, C. Wahlestedt, E. T. Liu, M. Harbers, J. Kawai, V. B. Bajic, D. A. Hume, Y. Hayashizaki, Genome-wide analysis of mammalian promoter architecture and evolution. *Nat Genet* **38**, 626-635 (2006).
28. H. Thorvaldsdottir, J. T. Robinson, J. P. Mesirov, Integrative Genomics Viewer (IGV): high-performance genomics data visualization and exploration. *Brief Bioinform* **14**, 178-192 (2013).
29. D. Pozzi, G. Lignani, E. Ferrea, A. Contestabile, F. Paonessa, R. D'Alessandro, P. Lippiello, D. Boido, A. Fassio, J. Meldolesi, F. Valtorta, F. Benfenati, P. Baldelli, REST/NRSF-mediated intrinsic homeostasis protects neuronal networks from hyperexcitability. *EMBO J* **32**, 2994-3007 (2013).
30. L. Breiman, *Random Forests*. Machine Learning (2001).

Acknowledgments: We thank Jenna Carpenter for the help with neuronal cultures and blinding, and Meena Siddharthana for the analysis of false negative with Pyecog. We are thankful to all members of the DCEE for helpful discussions.

Funding: This project was supported by the European Union's Horizon 2020 research and innovation program (Marie Skłodowska-Curie grant agreement no. 658418 to G.L.) and the Medical Research Council (MR/L01095X/1 to D.M.K. and S.S.).

Author contributions: G.C. and G.L performed the experiments and analysed data; C.D.B. designed and tested the sgRNAs and *Kcna1* transcriptional activation; Y.Q performed immunohistochemistry; L.M. developed the computational analysis; J.C creates the python script for EEG analysis and performed the automated analysis; A. S. developed python scripts for electrophysiology analysis; S.P.J helped in the development of the animal model; S. G. produced the homemade viruses; A.L. created and maintained the video-EEG setup; S.S, D.M.K., V.B. and G.L supervised, coordinated and supported the project and wrote the manuscript.

Competing interests: The authors declare no competing interests.

Data and materials availability: All the python scripts are freely available. Plasmids will be deposited in Addgene.

Supplementary Materials

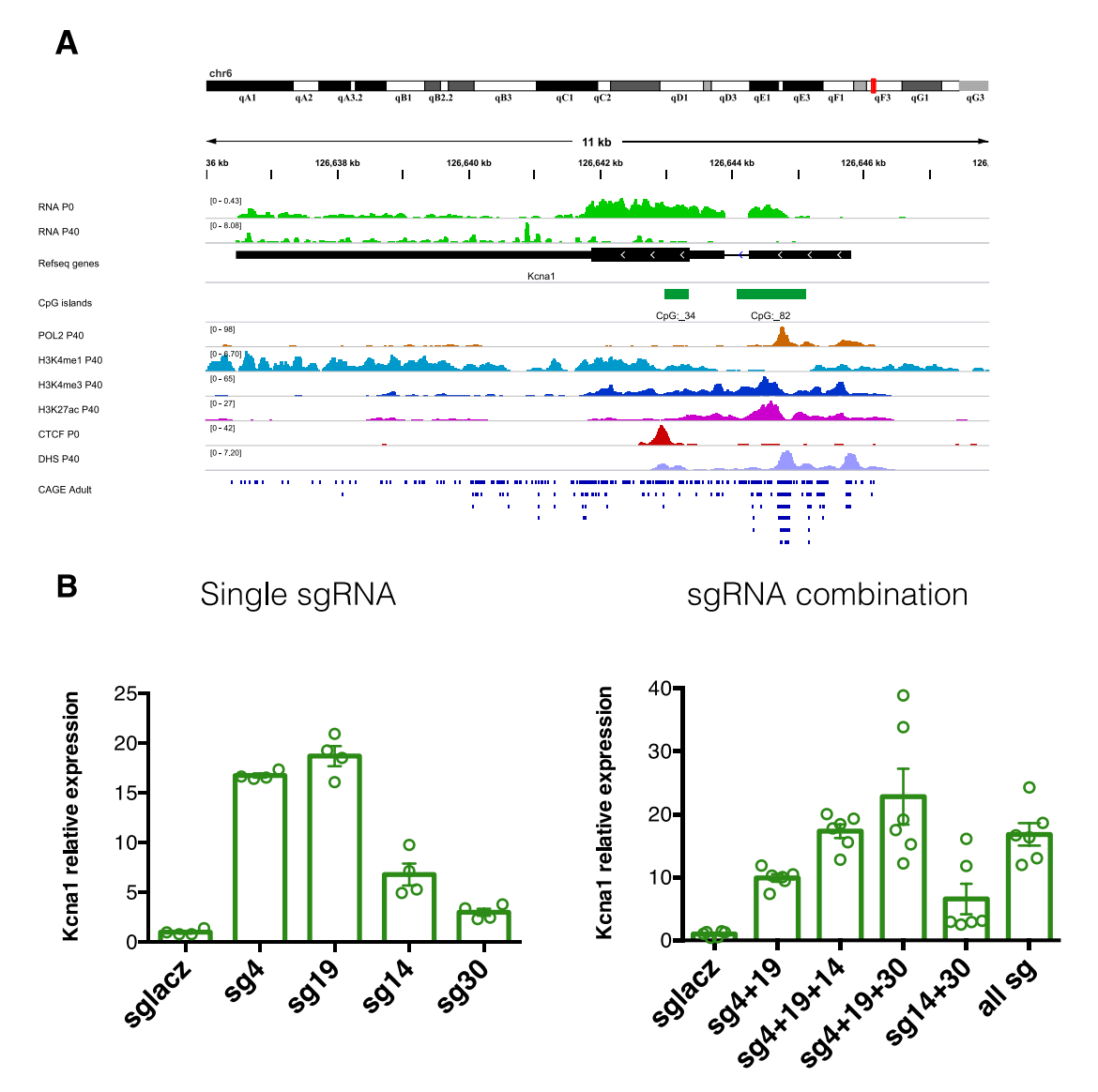

Figure S1: Bioinformatics analysis for prediction of *Kcna1* gene promoter and sgRNA screening for stimulating *Kcna1* gene expression with CRISPRa in P19 cells. A. Alignment of *Kcna1* gene reference sequence with RNA-seqs of mouse brain at P0 and P40, ChIP-seqs at P40 for POL2 (RNA polymerase II), H3K4me1 (mono-methylation of lysine 4 on histone H3), H3K4me3 (tri-methylation of lysine 4 on the histone H3) and H3K27ac (acetylation of lysine 27 on histone H3), CTCF (factor that binds the CCCTC) and DNase-seq (DHS, DNase I Hyper Sensitivity mapping) and CAGE- seq (Cap Analysis of Gene Expression-sequencing) profiles. The enrichment of markers associated with transcriptional

activation in the regions upstream to the first exon of the gene highlight the presence of a TSS and allows to localize a promoter region in the 200 bp upstream. **B**. RT-qPCRs for *Kcna1* mRNA levels on RNA extracted from P19 cells lipofected with dCas9VP160-T2A-Puro^{R} together with sgRNAs targeting Kcna1 gene promoter. Data are normalized on the 18S rRNA and relative to control sgLacZ cells.

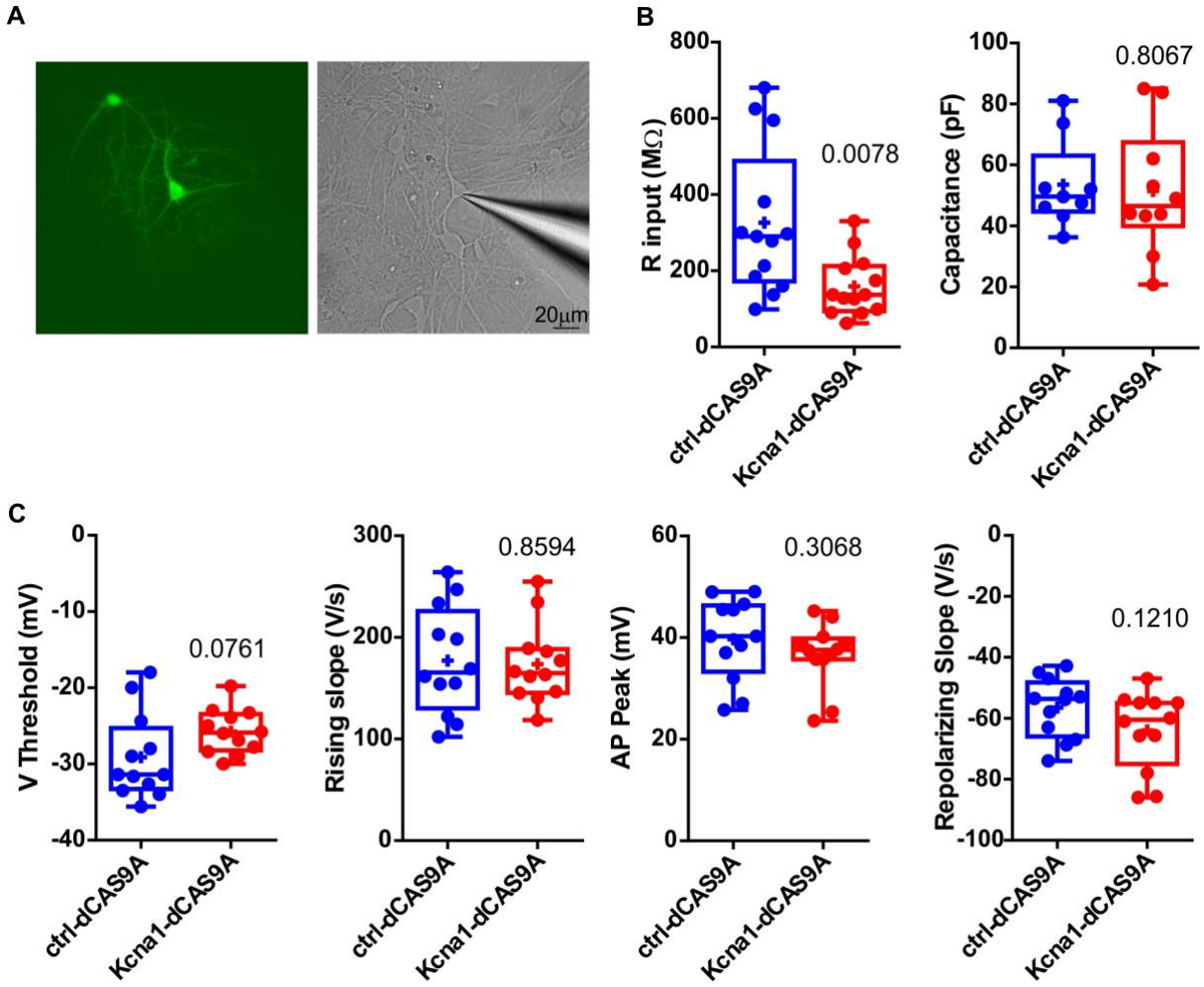

Figure S2: Electrophysiology recordings *in vitro.* Neuronal and AP parameters. A. representative picture of transduced patched neuron in vitro (Green= EGFP). **B, C.** Cell (B) and AP (C) parameters. Student's t test. Only the change in input resistance was significant for Ctrl-dCAS9A compared to Kcna1-dCAS9A neurons.

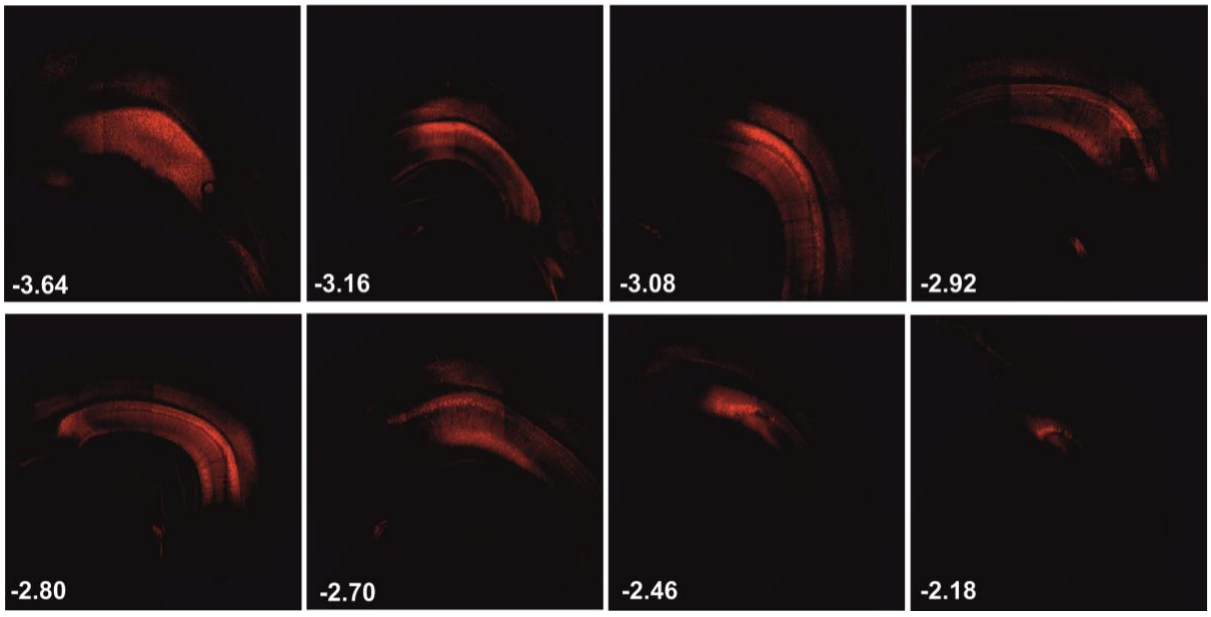

Figure S3: tdTomato expression in slices from Camk2a/CRE mouse. Representative images of slices from a Camk2a/CRE mouse injected with Ctrl-dCAS9A. Native tdTomato (non-immunofluorescence) was present in the floxed rtTa-t2a-tdTomato cassette driven by Syn promoter. Coordinates are from Bregma.

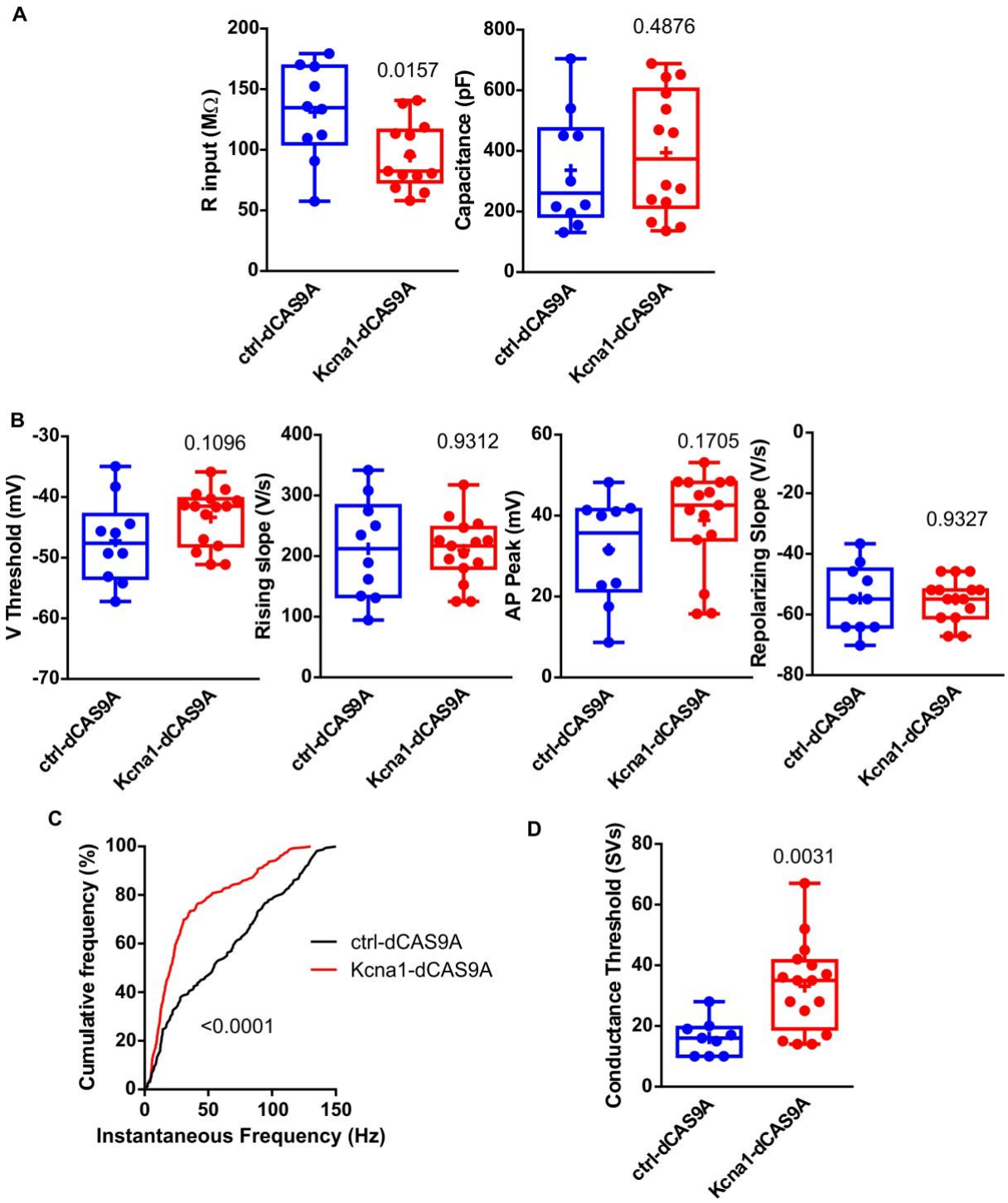

Figure S4: *Ex vivo* electrophysiological recordings in acute slices from Camk2a/CRE mice. A, B. Cell (B) and AP parameters. Student's t test. Only the input resistance was significant for Ctrl-dCAS9A compared to Kcna1-dCAS9A neurons. **C.** Cumulative analysis of instantaneous frequency for the first 2 APs in each current step for all neurons transduced either with Ctrl-dCAS9A or Kcna1-dCAS9A. Mann-Whitney non-parametric test. **D.**

Conductance threshold calculated as the first AP elicited with steps of single AMPA miniature events (*19*).

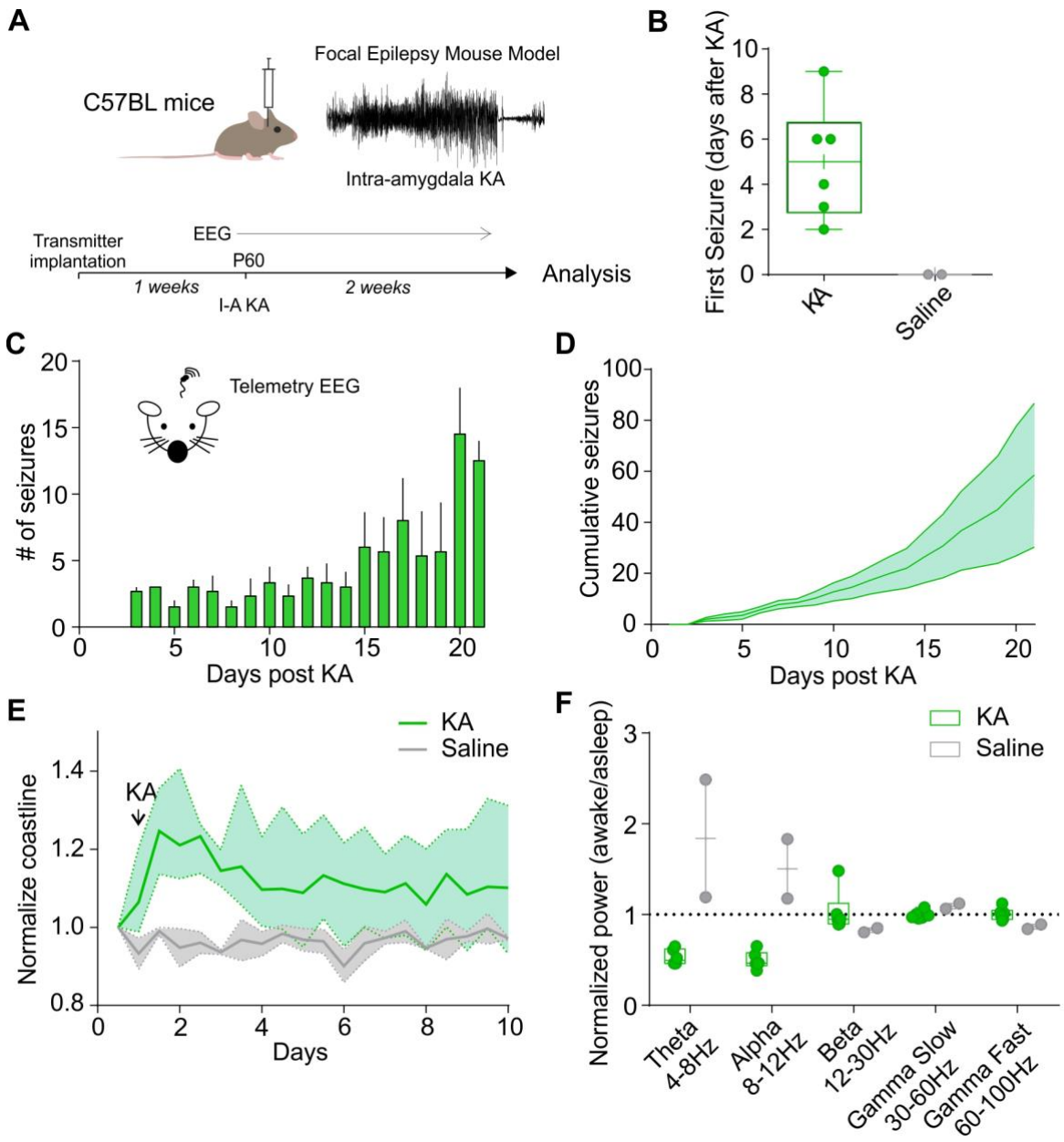

Figure S5: Intra-amygdala Kainic acid model of temporal lobe epilepsy. A. Experimental plan for inducing chronic epilepsy injecting KA in the right amygdala to induce status epilepticus (SE). **B.** Days after KA to show a stage 5 generalized tonic-clonic seizure in animals injected with KA in amygdala or saline. Average is 5 days after KA. **C, D.** Number of seizures (C) and cumulative number of seizures (D) in the first 3 weeks after KA injection (n=6). **E.** Coastline in the first 10 days after SE normalized to 12hrs EEG recordings before

SE for animals injected with KA (n=6) or saline (n=2). Data points are binned every 12hrs. **F.** Power during awake status (12hr night) normalized over asleep status (12hr day) for the theta, alpha, beta, slow and fast gamma bandwidths.

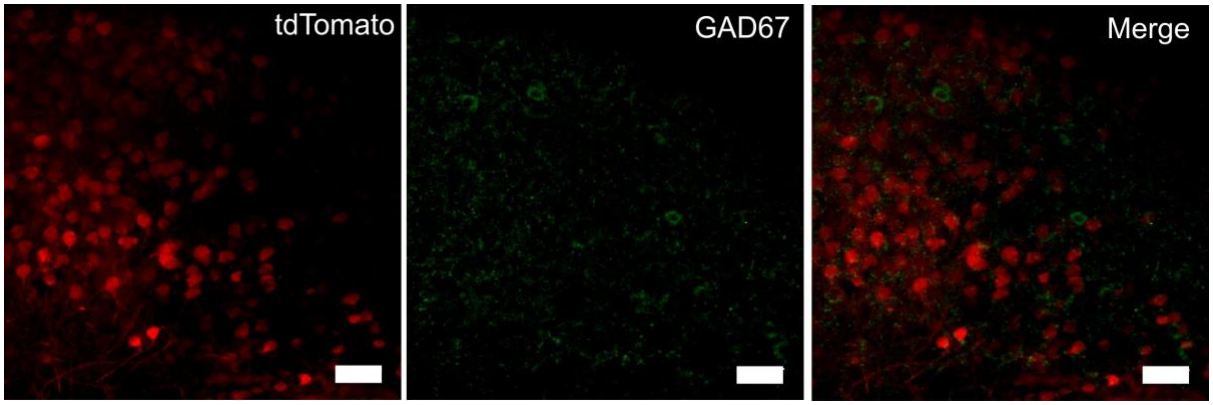

Figure S6: Immunohistochemistry of epileptic brains after the recordings.

Representative image of a ctrl-dCAS9A injected mouse where show no co-localization between tdTomato, driven by Camk2a promoter, and GAD67, marker for inhibitory neurons (scale bar: 50µm). No co-localisation between Camk2a and GAD67 was detected, in any of the 4 brains analysed after recordings.

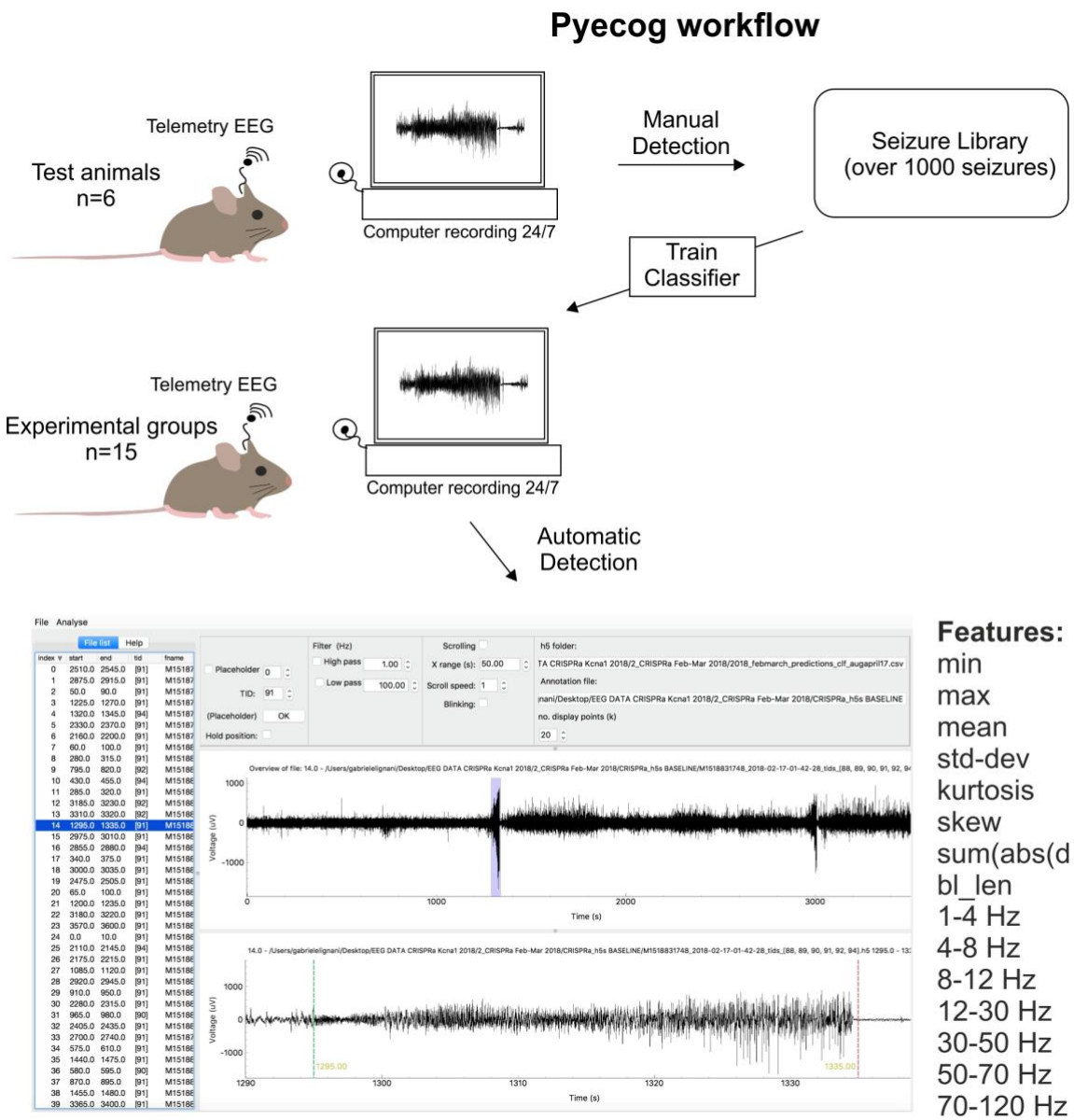

Figure S7: EEG analysis with Pyecog.